Electronic Supplementary Information

Self-assembly Co-doped MnO_2 nanorods networks with abundant oxygen vacancies modified separators for high-performance Li-S batteries

Chuyue Cai[1 §], Liping Wu[1 §], Zhiwei Cai[1], Fang Yu[2], Liu Zhang[2], Liya Wang[3], Tao Mei[1], Liangyou Lin[1], and Xianbao Wang[1,]*

[1]Hubei Collaborative Innovation Center for Advanced Organic Chemical Materials, Overseas, Expertise Introduction Center for Discipline Innovation (D18025), Key Laboratory for the Green Preparation and Application of Functional Materials, Hubei Key Laboratory of Polymer Materials, School of Materials Science and Engineering, Hubei University, Wuhan 430062, P.R. China

[2]School of Materials Science and Engineering, Yancheng Institute of Technology, Yancheng 224051, P.R. China

[3]School of Architecture, Southeast University, Nanjing 210096, P. R. China

§ These authors contributed equally to this work

* Corresponding author. Fax: +86 27 8866 1729; Tel.: +86 27 8866 2132.

E-mail: wxb@hubu.edu.cn (X.B. Wang)

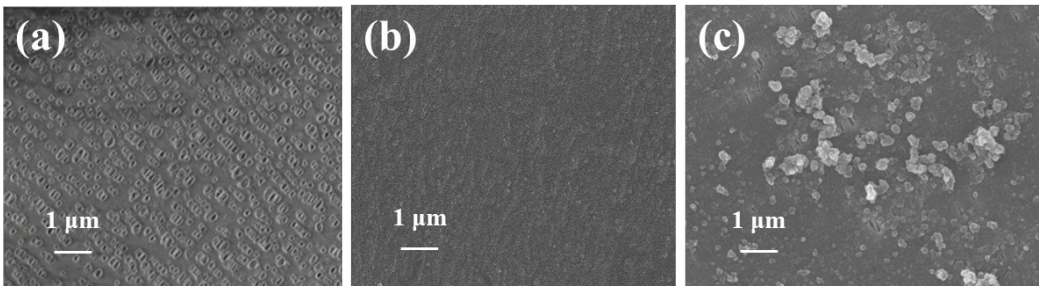

Fig. S1. SEM images of (a) PP separator, (b) Co-MnO_x@PP separator, and (c) MnO_2@PP separator.

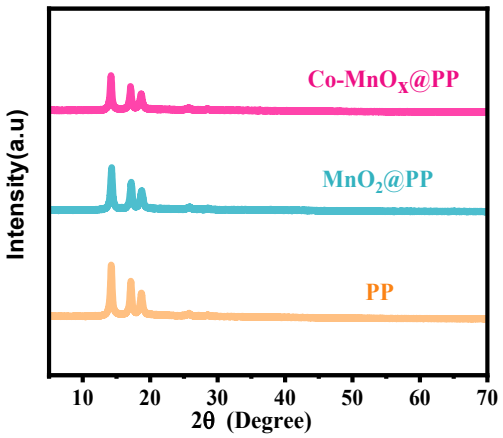

Fig. S2. XRD patterns of Co-MnO_x@PP, MnO_2@PP and PP separators.

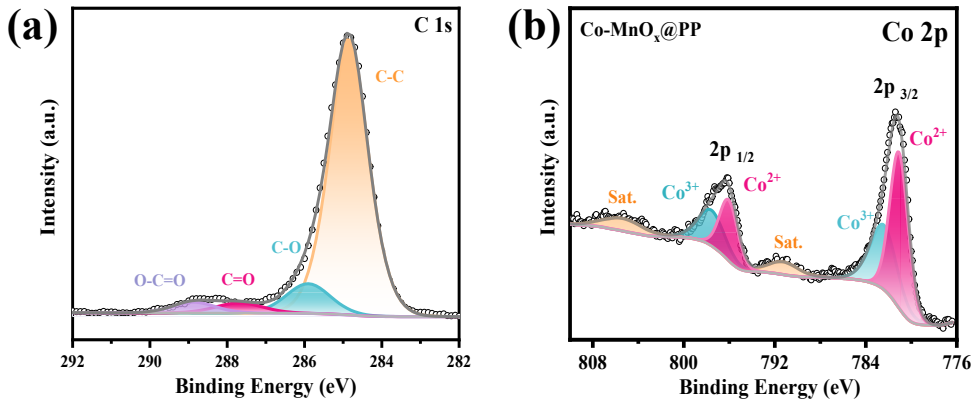

Fig. S3. XPS spectra of (a) C 1s, (b) Co 2p for Co-MnO_x@PP separators.

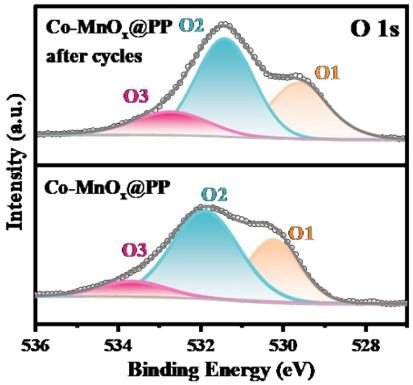

Fig. S4. XPS spectra of O 1s for Co-MnO_x@PP separators after cycles.

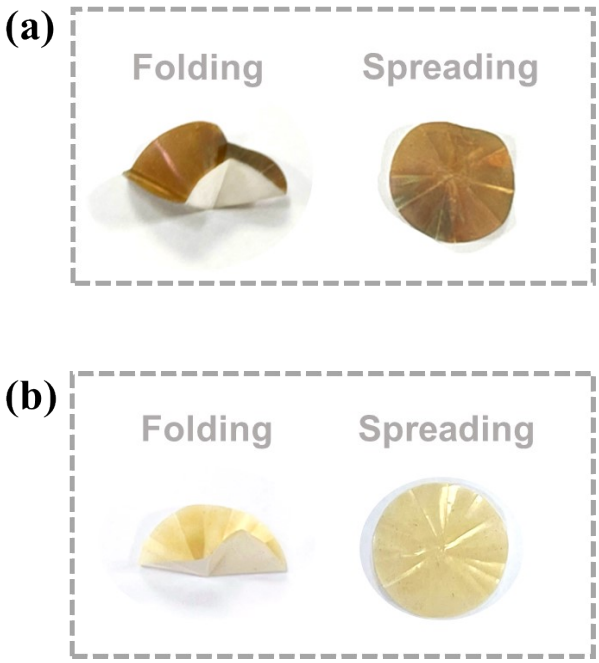

Fig. S5. Digital photographs of the folding and spreading test of (a) Co-MnO_x@PP and (b) MnO_2@PP separators.

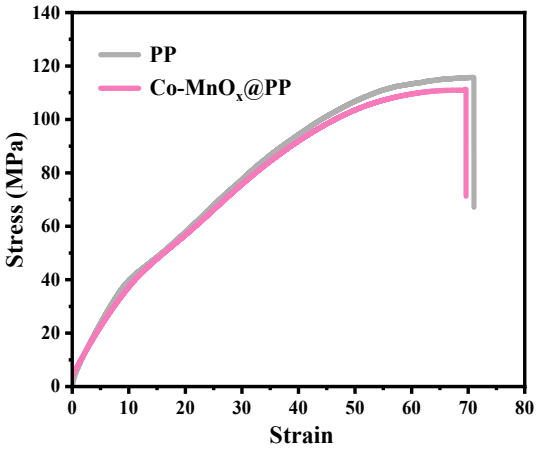

Fig. S6. Typical tensile stress-strain curves of commercial PP and Co-MnO_x@PP separators.

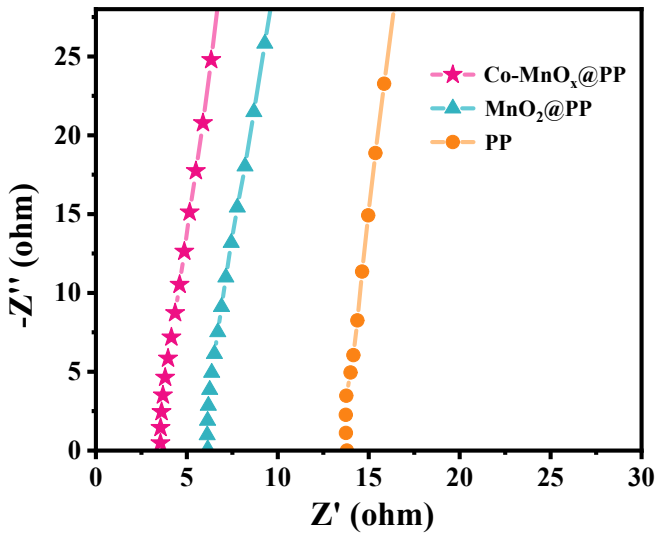

Fig. S7. EIS of the lithium symmetric cells with Co-MnO_x@PP, MnO_2@PP and PP separators.

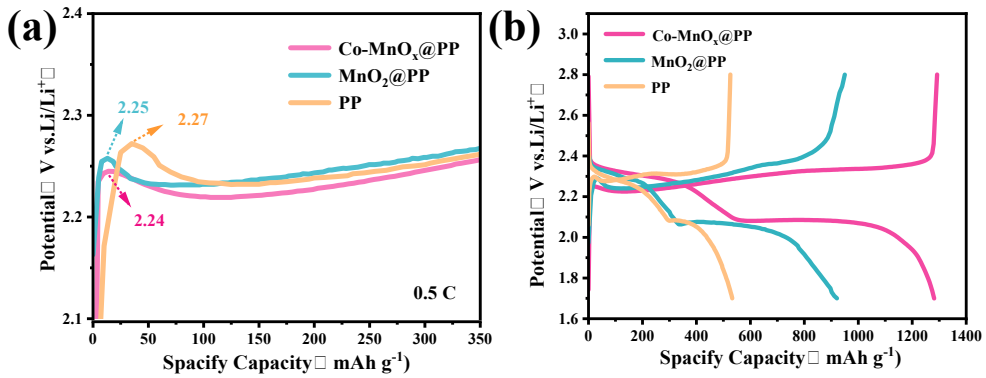

Fig. S8. (a) Initial and (b) whole charge/discharge curves of Li-S cells with Co-MnO_x@PP, MnO_2@PP and PP separators at 0.5 C.

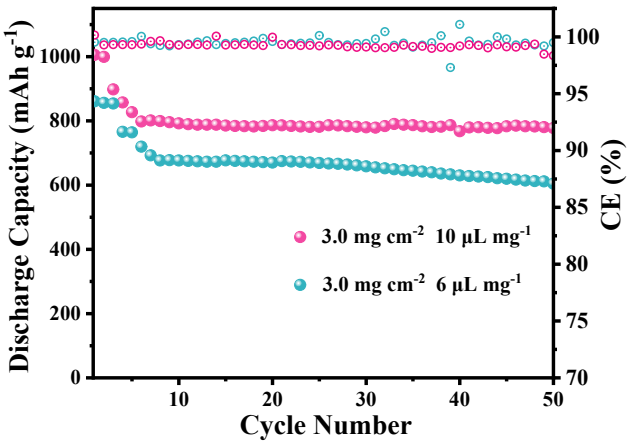

Fig. S9. The cycle of Co-MnO_x@PP modified separator under high sulfur loading and low E/S ratio

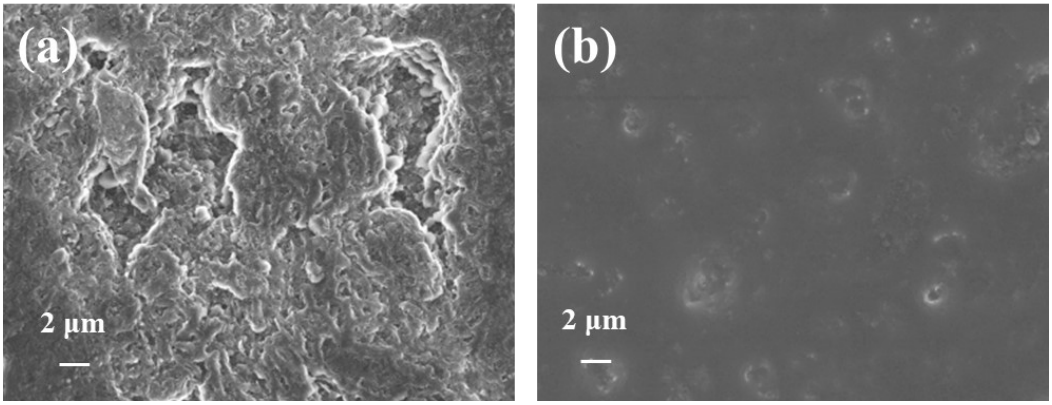

Fig. S10. SEM images of Li anode in contact with (a) PP and (b) Co-MnO_x@PP separators after 100 cycles.

Table S1. Summary of electrochemical performance of Li-S batteries configured with different modified separators and interlayers.

Modified separator	S loading (mg cm^{-2})	Reversible capacity (mAh g^{-1})	Capacity retention /cycle number/Rate	Ref.
MnO_2@PE	1.5	603	65 %/500/0.5 C	[1]
Fe_3O_4/RGO//PP	0.7-1.0	728	60%/400/1.8 C	[2]
Co_3O_4@GC/N-CNT NF-coated separator	2.0	389	59 %/500/0.5 C	[3]
MnO-OVs/NCNTs/PP	1.5	618	66 %/500/1 C	[4]
MnO_2 separator	1-1.2	494	71 %/500/0.5 C	[5]
Mn/Co–N–C separator	1.0	522	64 %/1000/2 C	[6]
$NiCo_2O_{4-x}$ modified separator	1.5	327	53 %/500/2.5 C	[7]
CSUST1/CNT_x0002 coated separator	2.0	708	58 %/600/1 C	[8]
Co-MnO_x@PP	1.6	902	84.4 %/200/0.5 C	This work
	1.6	715	65.3 %/500/3 C	
	3.0	777	78.8 %/50/0.5 C	

References

1. Song, X.; Chen, G.; Wang, S.; Huang, Y.; Jiang, Z.; Ding, L. X.; Wang, H. Self-Assembled Close-Packed MnO2 Nanoparticles Anchored on a Polyethylene Separator for Lithium-Sulfur Batteries. ACS Appl. Mater. Interfaces 2018, 10 (31), 26274-26282.

2. P. Cheng, P. Guo, D. Liu, Y. Wang, K. Sun, Y. Zhao, D. He, Fe3O4/RGO modified separators to suppress the shuttle effect for advanced lithium-sulfur cbatteries, J. Alloys Compd. 784 (2019) 149-156.

3. Saroha, R.; Oh, J. H.; Lee, J. S.; Kang, Y. C.; Jeong, S. M.; Kang, D.-W.; Cho, C.; Cho, J. S. Hierarchically porous nanofibers comprising multiple core–shell Co3O4@graphitic carbon nanoparticles grafted within N-doped CNTs as functional interlayers for excellent Li–S batteries. Chem. Eng. J. 2021, 426.

4. Yu, X.; Chen, W.; Cai, J.; Lu, X.; Sun, Z. Oxygen vacancy-rich MnO nanoflakes/N-doped carbon nanotubes modified separator enabling chemisorption and catalytic conversion of polysulfides for Li-S batteries. J. Colloid Interface Sci. 610(2022), 407-417

5. Wang, X.; Yang, L.; Wang, Y.; Li, Q.; Chen, C.; Zhong, B.; Chen, Y.; Guo, X.; Wu, Z.; Liu, Y.; Liu, Y.; Sun, Y. Novel functional separator with self-assembled MnO2 layer via a simple and fast method in lithium-sulfur battery. J. Colloid Interface Sci. 606 (1) (2022), 666-676.

6. Qiao, S.; Wang, Q.; Lei, D.; Shi, X.; Zhang, Q.; Huang, C.; Liu, A.; He, G.; Zhang, F. Oxygen vacancy enabled fabrication of dual-atom Mn/Co catalysts for high-

performance lithium-sulfur batteries. J. Mater. Chem. A 10 (21) (2022, 11702-11711.

7. Zhu, Y.; Zuo, Y.; Ye, F.; Zhou, J.; Tang, Y.; Chen, Y. Dual-regulation strategy to enhance electrochemical catalysis ability of NiCo2O4-x for polysulfides conversion in Li-S batteries. Chem. Eng. J. 2022, 428.

8. Jin, H. G.; Wang, M.; Wen, J. X.; Han, S. H.; Hong, X. J.; Cai, Y. P.; Li, G.; Fan, J.; Chao, Z. S. Oxygen Vacancy-Rich Mixed-Valence Cerium MOF: An Efficient Separator Coating to High-Performance Lithium-Sulfur Batteries. ACS Appl. Mater. Interfaces 13 (3) (2021), 3899-3910.